

This is the accepted manuscript made available via CHORUS. The article has been published as:

## Radiative resonance couplings in $\gamma\pi\rightarrow\pi\pi$

Martin Hoferichter, Bastian Kubis, and Marvin Zanke

Phys. Rev. D **96**, 114016 — Published 14 December 2017

DOI: [10.1103/PhysRevD.96.114016](https://doi.org/10.1103/PhysRevD.96.114016)

# Radiative resonance couplings in $\gamma\pi \rightarrow \pi\pi$

Martin Hoferichter,<sup>1</sup> Bastian Kubis,<sup>2,3</sup> and Marvin Zanke<sup>2</sup>

<sup>1</sup>*Institute for Nuclear Theory, University of Washington, Seattle, WA 98195-1550, USA*

<sup>2</sup>*Helmholtz-Institut für Strahlen- und Kernphysik (Theorie), Universität Bonn, D-53115 Bonn, Germany*

<sup>3</sup>*Bethe Center for Theoretical Physics, Universität Bonn, D-53115 Bonn, Germany*

Studies of the reaction  $\gamma\pi \rightarrow \pi\pi$ , in the context of the ongoing Primakoff program of the COMPASS experiment at CERN, give access to the radiative couplings of the  $\rho(770)$  and  $\rho_3(1690)$  resonances. We provide a vector-meson-dominance estimate of the respective radiative width of the  $\rho_3$ ,  $\Gamma_{\rho_3 \rightarrow \pi\gamma} = 48(18)$  keV, as well as its impact on the  $F$ -wave in  $\gamma\pi \rightarrow \pi\pi$ . For the  $\rho(770)$ , we establish the formalism necessary to extract its radiative coupling directly from the residue of the resonance pole by analytic continuation of the  $\gamma\pi \rightarrow \pi\pi$  amplitude to the second Riemann sheet, without any reference to the vector-meson-dominance hypothesis.

PACS numbers: 11.55.Fv, 13.75.Lb, 11.30.Rd, 13.60.Le

Keywords: Dispersion relations, Meson-meson interactions, Chiral Symmetries, Meson production

## I. INTRODUCTION

Apart from the two-photon decay of the neutral pion, the process  $\gamma\pi \rightarrow \pi\pi$  is the simplest manifestation of the Wess–Zumino–Witten anomaly [1, 2]. The leading order in the chiral expansion [3–5],

$$F_{3\pi} = \frac{eN_c}{12\pi^2 F_\pi^3} = 9.76(3) \text{ GeV}^{-3}, \quad (1)$$

is determined by the number of colors  $N_c$ , the electric charge  $e = \sqrt{4\pi\alpha}$ , and the pion decay constant  $F_\pi = 92.28(9) \text{ MeV}$  [6]. Given that early measurements, most prominently  $F_{3\pi} = 12.9(1.0) \text{ GeV}^{-3}$  [7], suggested some tension with the low-energy theorem, corrections beyond the leading order (1) have been worked out [8–13], with the net result that higher-order and electromagnetic corrections reduce the value to  $F_{3\pi} = 10.7(1.2) \text{ GeV}^{-3}$ . Together with a similar extraction from  $\pi^- e^- \rightarrow \pi^- e^- \pi^0$  [14], leading to  $F_{3\pi} = 9.6(1.1) \text{ GeV}^{-3}$ , the low-energy theorem is now tested at the 10% level, far behind the 1.5%-level accuracy that has been reached in  $\pi^0 \rightarrow \gamma\gamma$  [15, 16]. Meanwhile, a first lattice calculation of  $\gamma^* \pi \rightarrow \pi\pi$  has been reported in [17, 18].

In contrast to earlier measurements, the Primakoff studies at COMPASS cover not only the threshold region of  $\gamma\pi \rightarrow \pi\pi$ , but extend to much higher center-of-mass energies. As pointed out in [19], this allows one to use the  $\rho$  resonance as a lever to vastly increase the statistics of the anomaly extraction, combining constraints from analyticity, unitarity, and crossing symmetry into a two-parameter description of the amplitude whose normalization coincides with  $F_{3\pi}$ . More recently, interest in the  $\gamma\pi \rightarrow \pi\pi$  reaction has been triggered by its relation to the hadronic-light-by-light contribution to the anomalous magnetic moment of the muon, where it appears as a crucial input quantity for a data-driven determination of the  $\pi^0 \rightarrow \gamma^* \gamma^*$  transition form factor [20], which in turn determines the strength of the pion-pole contribution in a dispersive approach to hadronic light-by-light scattering [21–25].

In fact, the kinematic reach of the COMPASS experiment extends up to and including the  $\rho_3(1690)$ , the first resonance in the  $F$ -wave. In this paper, we estimate its impact on the  $\gamma\pi \rightarrow \pi\pi$  cross section based on vector-meson-dominance (VMD) assumptions, which corresponds to an estimate of the radiative width  $\Gamma_{\rho_3 \rightarrow \pi\gamma}$ , see Sect. II. For the  $\rho(770)$  such a simplified approach is not adequate anymore, precisely due to the amount of statistics available at the  $\rho$  peak that should allow one to significantly sharpen the test of the chiral low-energy theorem in the future [26]. Instead, the analytic continuation of the  $\gamma\pi \rightarrow \pi\pi$  amplitudes that underlie this extraction, in combination with the known  $\rho$ -pole parameters and residues from  $\pi\pi$  scattering [27, 28], determines the  $\rho\pi\gamma$  coupling constant,  $g_{\rho\pi\gamma}$ , once the free parameters of the representation have been fit to the cross section. The precise prescription how to extract the radiative coupling of the  $\rho$ , defined through the residue of the pole in a model-independent way, is spelled out in Sect. III. Combining all currently available information, prior to the direct COMPASS measurement, we predict the line shape of the cross section in Sect. IV. A short summary is provided in Sect. V.

## II. VECTOR MESON DOMINANCE

Throughout, we follow the conventions of [19]. The amplitude for the process

$$\gamma(q)\pi^-(p_1) \rightarrow \pi^-(p_2)\pi^0(p_0) \quad (2)$$

is decomposed according to

$$\mathcal{M}_{\gamma\pi \rightarrow \pi\pi}(s, t, u) = i\epsilon_{\mu\nu\alpha\beta}\epsilon^\mu p_1^\nu p_2^\alpha p_0^\beta \mathcal{F}(s, t, u), \quad (3)$$

in terms of the scalar function  $\mathcal{F}(s, t, u)$ , the photon polarization vector  $\epsilon^\mu$ , and Mandelstam variables chosen as  $s = (q + p_1)^2$ ,  $t = (p_1 - p_2)^2$ , and  $u = (p_1 - p_0)^2$ , with  $s + t + u = 3M_\pi^2$ , particle masses defined by the charged states, and a relation to the center-of-mass scattering an-

gle  $z = \cos \theta$  according to

$$\begin{aligned} t &= a(s) + b(s)z, & u &= a(s) - b(s)z, \\ a(s) &= \frac{3M_\pi^2 - s}{2}, & b(s) &= \frac{s - M_\pi^2}{2}\sigma_\pi(s), \\ \sigma_\pi(s) &= \sqrt{1 - \frac{4M_\pi^2}{s}}. \end{aligned} \quad (4)$$

Crossing symmetry implies that the scalar function  $\mathcal{F}(s, t, u)$  is fully symmetric in  $s, t, u$ . In the conventions of (3) the cross section becomes

$$\sigma(s) = \frac{(s - 4M_\pi^2)^{3/2}(s - M_\pi^2)}{1024\pi\sqrt{s}} \int_{-1}^1 dz (1 - z^2) |\mathcal{F}(s, t, u)|^2. \quad (5)$$

Later, we also need the partial-wave decomposition [29]

$$\mathcal{F}(s, t, u) = \sum_{\text{odd } l} f_l(s) P'_l(z), \quad (6)$$

where  $P'_l(z)$  denotes the derivative of the Legendre polynomials, and the inversion is given by

$$f_l(s) = \frac{1}{2} \int_{-1}^1 dz (P_{l-1}(z) - P_{l+1}(z)) \mathcal{F}(s, t, u). \quad (7)$$

Elastic unitarity relates these partial waves to the isospin  $I = 1$   $\pi\pi$  phase shifts  $\delta_l^1(s)$ ,

$$\begin{aligned} \mathcal{M}_{\pi\pi}^{I=1}(s, t) &= 32\pi \sum_{\text{odd } l} (2l+1) t_l^1(s) P_l \left( 1 + \frac{2t}{s - 4M_\pi^2} \right), \\ t_l^1(s) &= \frac{e^{2i\delta_l^1(s)} - 1}{2i\sigma_\pi(s)}, \end{aligned} \quad (8)$$

by means of

$$\text{Im } f_l(s) = \sigma_\pi(s) (t_l^1(s))^* f_l(s) \theta(s - 4M_\pi^2). \quad (9)$$

The fact that the phase of  $f_l(s)$  coincides with  $\delta_l^1(s)$  is a manifestation of Watson's final-state theorem [30]. Finally, the dominant electromagnetic correction [12] amounts to

$$\mathcal{F}(s, t, u) \rightarrow \mathcal{F}(s, t, u) - \frac{2e^2 F_\pi^2}{t} F_{3\pi}. \quad (10)$$

### A. $\rho(770)$

The VMD amplitude for  $\gamma\pi \rightarrow \pi\pi$  can be constructed by combining the  $\rho \rightarrow \pi\pi$  amplitude from

$$\mathcal{L}_{\rho\pi\pi} = g_{\rho\pi\pi} \epsilon^{abc} \pi^a \partial^\mu \pi^b \rho_\mu^c, \quad (11)$$

with isospin indices  $a, b, c$ , together with

$$\mathcal{M}_{\rho\pi\gamma} = e g_{\rho\pi\gamma} \epsilon_{\mu\nu\alpha\beta} \epsilon_\rho^\mu \epsilon_\gamma^\nu p_1^\alpha p_2^\beta, \quad (12)$$

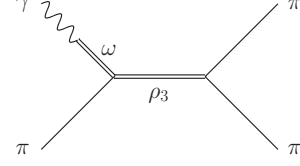


FIG. 1: VMD mechanism for the  $\rho_3$  contribution to  $\gamma\pi \rightarrow \pi\pi$ .

where  $p_1$  and  $p_2$  refer to the momenta of the pion and the photon, and  $\epsilon_\rho^\mu, \epsilon_\gamma^\nu$  to the  $\rho$  and  $\gamma$  polarization vectors. The result reads

$$f_1^{\text{VMD}}(s) = \frac{2e g_{\rho\pi\gamma} g_{\rho\pi\pi}}{M_\rho^2 - iM_\rho \Gamma_\rho - s}, \quad (13)$$

where the finite width of the  $\rho$  has been taken into account by means of a Breit–Wigner propagator. In Sect. III we will reinterpret both couplings,  $g_{\rho\pi\pi}$  and  $g_{\rho\pi\gamma}$ , as residues of the respective poles, but for the moment we first collect the phenomenological information available when treating the  $\rho$  as a narrow resonance. In this approximation, the width becomes

$$\Gamma_{\rho \rightarrow \pi\pi} = \frac{|g_{\rho\pi\pi}|^2}{48\pi M_\rho^2} (M_\rho^2 - 4M_\pi^2)^{3/2}, \quad (14)$$

i.e.  $|g_{\rho\pi\pi}| \sim 5.95(2)$ , with masses and widths as listed in [6] (accounting for the different phase space, the results for charged and neutral channels are virtually identical). Similarly, the radiative decay width becomes

$$\Gamma_{\rho \rightarrow \pi\gamma} = \frac{e^2 |g_{\rho\pi\gamma}|^2}{96\pi M_\rho^3} (M_\rho^2 - M_\pi^2)^3. \quad (15)$$

Within the narrow-width approximation, one could then extract  $|g_{\rho\pi\gamma}|$  from the measured cross section for  $\gamma\pi \rightarrow \pi\pi$  and thereby determine  $\Gamma_{\rho \rightarrow \pi\gamma}$ . At a similar level of accuracy,  $SU(3)$  symmetry (see e.g. [31]) suggests  $\Gamma_{\rho \rightarrow \pi\gamma} = \Gamma_{\omega \rightarrow \pi^0\gamma}/9 = 79(2) \text{ keV}$ , indeed close to  $\Gamma_{\rho^0 \rightarrow \pi^0\gamma} = 69(9) \text{ keV}$ ,  $\Gamma_{\rho^\pm \rightarrow \pi^\pm\gamma} = 68(7) \text{ keV}$  [6]. A model-independent extraction of the radiative coupling of the  $\rho$  from  $\gamma\pi \rightarrow \pi\pi$  will be discussed in Sect. III.

### B. $\rho_3(1690)$

For the generalization to the  $\rho_3(1690)$  contribution to  $\gamma\pi \rightarrow \pi\pi$  and the determination of its radiative width, we follow [32, 33]. To this end, we first remark that  $G$ -parity dictates the photon in this process to have isoscalar quantum numbers. In the VMD picture, it therefore couples to the  $\rho_3$  and a pion predominantly via the  $\omega$  meson (assuming the  $\phi$  to be negligible due to OZI suppression). As we aim for a *prediction* of the radiative decay of the  $\rho_3$ , we in particular need to assume *strict* VMD without a direct  $\rho_3\pi\gamma$  coupling. Figure 1 therefore suggests

that we need to determine the coupling constants  $g_{\rho_3\pi\pi}$ ,  $g_{\rho_3\pi\omega}$ , as well as  $g_{\omega\gamma}$ .

Starting from [33]

$$\begin{aligned}\mathcal{L}_{\rho_3} &= \frac{g_{\rho_3\pi\pi}}{4F_\pi^2} \langle \rho_{\mu\nu\lambda} [\partial^\mu \pi, \partial^\nu \partial^\lambda \pi] \rangle \\ &\quad + \frac{g_{\rho_3\pi\omega}}{2F_\pi} \epsilon^{\lambda\alpha\beta\gamma} \langle \rho_{\mu\nu\lambda} \partial^\mu \partial_\alpha \pi \rangle \partial^\nu \partial_\beta \omega_\gamma, \\ \mathcal{L}_{\omega\gamma} &= -\frac{eM_\omega^2}{g_{\omega\gamma}} A^\mu \omega_\mu,\end{aligned}\quad (16)$$

with spin-3 fields  $\rho_{\mu\nu\lambda} = \rho_{\mu\nu\lambda}^a \tau^a$ , pion isotriplet  $\pi = \pi^a \tau^a$ , the isoscalar vector field  $\omega_\mu$ , and the electromagnetic field  $A_\mu$ , one finds the partial decay widths

$$\begin{aligned}\Gamma_{\rho_3 \rightarrow \pi\pi} &= \frac{|g_{\rho_3\pi\pi}|^2}{4480\pi F_\pi^4 M_{\rho_3}^2} (M_{\rho_3}^2 - 4M_\pi^2)^{7/2}, \\ \Gamma_{\rho_3 \rightarrow \pi\omega} &= \frac{|g_{\rho_3\pi\omega}|^2}{13440\pi F_\pi^2 M_{\rho_3}^7} \lambda(M_{\rho_3}^2, M_\omega^2, M_\pi^2)^{7/2},\end{aligned}\quad (17)$$

where  $\lambda(x, y, z) = x^2 + y^2 + z^2 - 2(xy + xz + yz)$ . Together with  $M_{\rho_3} = 1688.8(2.1)$  MeV,  $\Gamma_{\rho_3} = 161(10)$  MeV,  $\text{BR}(\rho_3 \rightarrow \pi\pi) = 23.6(1.3)\%$ , and  $\text{BR}(\rho_3 \rightarrow \pi\omega) = 16(6)\%$  [6] this fixes the parameters according to

$$|g_{\rho_3\pi\pi}| = 0.056(2), \quad |g_{\rho_3\pi\omega}| = 1.2(2) \text{ GeV}^{-2}. \quad (18)$$

Similarly, one then finds for the radiative width

$$\Gamma_{\rho_3 \rightarrow \pi\gamma} = \frac{e^2 |g_{\rho_3\pi\omega}|^2}{13440\pi F_\pi^2 |g_{\omega\gamma}|^2 M_{\rho_3}^7} (M_{\rho_3}^2 - M_\pi^2)^7, \quad (19)$$

and with  $|g_{\omega\gamma}| = 16.7(2)$  extracted from

$$\Gamma_{\omega \rightarrow e^+ e^-} = \frac{e^4 (M_\omega^2 - 4m_e^2)^{1/2}}{12\pi |g_{\omega\gamma}|^2} \left( 1 + \frac{2m_e^2}{M_\omega^2} \right), \quad (20)$$

we obtain the prediction

$$\Gamma_{\rho_3 \rightarrow \pi\gamma} = 48(18) \text{ keV}. \quad (21)$$

This result lies slightly higher than the quark-model estimate  $\Gamma_{\rho_3 \rightarrow \pi\gamma} = 21 \text{ keV}$  [34]. Finally, the resonant contribution to the  $\gamma\pi \rightarrow \pi\pi$   $F$ -wave becomes

$$f_3^{\text{VMD}}(s) = \frac{eg_{\rho_3\pi\pi}g_{\rho_3\pi\omega}(s - 4M_\pi^2)(s - M_\pi^2)^2}{60F_\pi^3 g_{\omega\gamma} s (M_{\rho_3}^2 - iM_{\rho_3}\Gamma_{\rho_3} - s)}. \quad (22)$$

### III. RADIATIVE COUPLING OF THE $\rho(770)$

#### A. $\pi\pi$ scattering

In a model-independent way, the properties of the  $\rho(770)$  are encoded in the pole position and residues of the  $S$ -matrix on the second Riemann sheet. The prime process to determine the parameters is  $I = 1$   $\pi\pi$  scattering, whose partial-wave amplitude in the vicinity of the pole can be written as

$$t_{1,\text{II}}^1(s) = \frac{g_{\rho\pi\pi}^2 (s - 4M_\pi^2)}{48\pi(s_\rho - s)}, \quad s_\rho = \left( M_\rho - i\frac{\Gamma_\rho}{2} \right)^2, \quad (23)$$

Ref.	$M_\rho$ [MeV]	$\Gamma_\rho$ [MeV]	$ g_{\rho\pi\pi} $	$\arg(g_{\rho\pi\pi})$ [40]
[28], GKP	$763.7_{-1.5}^{+1.7}$	$146.4_{-2.2}^{+2.0}$	$6.01_{-0.07}^{+0.04}$	$(-5.3_{-0.6}^{+1.0})^\circ$
[28], Roy	$761_{-3}^{+4}$	$143.4_{-4.6}^{+3.8}$	$5.95_{-0.08}^{+0.12}$	$(-5.7_{-1.4}^{+1.1})^\circ$
[27], Roy	$762.4(1.8)$	$145.2(2.8)$		

TABLE I: Pole parameters of the  $\rho(770)$  from dispersion relations. The phase  $\arg(g_{\rho\pi\pi})$  in the last column is only determined modulo  $180^\circ$ .

where the conventions have been chosen in such a way that in the narrow-width limit the coupling  $g_{\rho\pi\pi}$  matches onto the Lagrangian definition (11). Elastic unitarity for  $\pi\pi$  scattering relates the amplitudes on the first and second Riemann sheets according to

$$t_{1,\text{I}}^1(s) - t_{1,\text{II}}^1(s) = -2\sigma^\pi(s) t_{1,\text{I}}^1(s) t_{1,\text{II}}^1(s), \quad (24)$$

where we have introduced [35]

$$\sigma^\pi(s) = \sqrt{\frac{4M_\pi^2}{s} - 1}, \quad \sigma^\pi(s \pm i\epsilon) = \mp i\sigma^\pi(s), \quad (25)$$

so that the pole parameters can be determined from the condition that  $t_{1,\text{I}}^1(s_\rho) = 1/(2\sigma^\pi(s_\rho)) = -i/(2\sigma_\pi(s_\rho))$  (since  $\text{Im } s_\rho < 0$ ), once a reliable representation of  $t_{1,\text{I}}^1(s)$  on the first sheet is available. Such a representation is provided by dispersion relations, in the form of Roy equations [36–38] or variants thereof, the so-called GKP equations [39]. The latter produce the pole parameters given in the first line of Table I, in good agreement with the determination from Roy equations, but with smaller uncertainties. In the following, we use the GKP parameters from [28] together with the  $I = 1$  phase shifts from [39]. Within uncertainties, this covers similar determinations listed in the table. Note that  $g_{\rho\pi\pi}$  is a *complex* coupling, with a phase that is observable (modulo  $180^\circ$ ), although Table I shows that this phase is rather small [40].

#### B. Pion form factor

The simplest quantity that probes the electromagnetic interactions of the pion is its form factor  $F_\pi^V(s)$ . Given the wealth of experimental data, it provides an ideal testing ground to study how well VMD predictions fare when confronted with real data, in this case for  $g_{\rho\gamma}$  instead of  $g_{\rho\pi\gamma}$ . In analogy to (24), the elastic unitarity relation,

$$\text{Im } F_\pi^V(s) = \sigma_\pi(s) (t_{1,\text{I}}^1(s))^* F_\pi^V(s) \theta(s - 4M_\pi^2), \quad (26)$$

defines the analytic continuation of the form factor onto the second sheet

$$F_{\pi,\text{I}}^V(s) - F_{\pi,\text{II}}^V(s) = -2\sigma^\pi(s) F_{\pi,\text{I}}^V(s) t_{1,\text{II}}^1(s). \quad (27)$$

In the vicinity of the pole we may write

$$F_{\pi,\text{II}}^V(s) = \frac{g_{\rho\pi\pi}}{g_{\rho\gamma}} \frac{s_\rho}{s_\rho - s}, \quad (28)$$

where the conventions are chosen in such a way that in the narrow-width and  $SU(3)$  limit  $g_{\rho\gamma} = g_{\omega\gamma}/3$ , cf. (16). Altogether one finds

$$\frac{1}{g_{\rho\gamma}g_{\rho\pi\pi}} = i\frac{\sigma_\pi^3(s_\rho)}{24\pi}F_{\pi,I}^V(s_\rho), \quad (29)$$

which allows one to extract  $g_{\rho\gamma}$  from the form factor evaluated at  $s_\rho$  on the first sheet and the previously determined  $g_{\rho\pi\pi}$ . The dispersive formalism for the analytic continuation to  $s_\rho$  has been studied in detail in the literature, see [25, 41–49], and data abound, mostly motivated by the  $\pi\pi$  contribution to hadronic vacuum polarization in the anomalous magnetic moment of the muon. In this way, the dominant uncertainties actually arise from the error in  $g_{\rho\pi\pi}$  as well as the systematics of the fit, e.g. whether  $\rho$ - $\omega$  mixing (as present in the fit to  $e^+e^-$  data [50–55], but not in  $\tau \rightarrow \pi\pi\nu$  [56]) is included in the definition of the form factor.

In the end, the results of the fits fall within the range  $|g_{\rho\gamma}| = 4.9(1)$ , so that, in this case, the VMD expectation,  $|g_{\rho\gamma}^{\text{VMD}}| = |g_{\omega\gamma}|/3 = 5.6(1)$ , agrees with the full result at the 10% level (strict VMD as derived from  $\rho \rightarrow e^+e^-$  in analogy to (20), without  $SU(3)$  assumptions, even produces  $|g_{\rho\gamma}^{\text{VMD}}| = 5.0$ ). The phase comes out around  $\arg(g_{\rho\pi\pi}g_{\rho\gamma}) \sim -7^\circ$ , so that  $g_{\rho\gamma}$  is almost real (with the same sign as the one chosen for  $g_{\rho\pi\pi}$ ).

### C. $\gamma\pi \rightarrow \pi\pi$

The derivation for  $\gamma\pi \rightarrow \pi\pi$  proceeds in close analogy to the pion form factor. From the unitarity relation (9) we find the analytic continuation

$$f_{1,I}(s) - f_{1,II}(s) = -2\sigma^\pi(s)f_{1,I}(s)t_{1,II}^1(s), \quad (30)$$

and writing

$$f_{1,II}(s) = \frac{2eg_{\rho\pi\gamma}g_{\rho\pi\pi}}{s_\rho - s} \quad (31)$$

in the vicinity of the pole (to match onto (13) in the VMD limit), the analog of (29) becomes

$$\frac{eg_{\rho\pi\gamma}}{g_{\rho\pi\pi}} = i\frac{s_\rho\sigma_\pi^3(s_\rho)}{48\pi}f_{1,I}(s_\rho). \quad (32)$$

However, the analytic continuation is less straightforward than for  $F_\pi^V(s)$ , due to the fact that, in contrast to the form factor, the scattering process  $\gamma\pi \rightarrow \pi\pi$  produces a left-hand cut, which, in addition, needs to be constructed in such a way that crossing symmetry is maintained. The corresponding formalism has been derived in [19]. Starting from the decomposition

$$\mathcal{F}(s, t, u) = \mathcal{F}(s) + \mathcal{F}(t) + \mathcal{F}(u), \quad (33)$$

which holds if imaginary parts from partial waves with  $l \geq 3$  are neglected, it was shown that the solution of

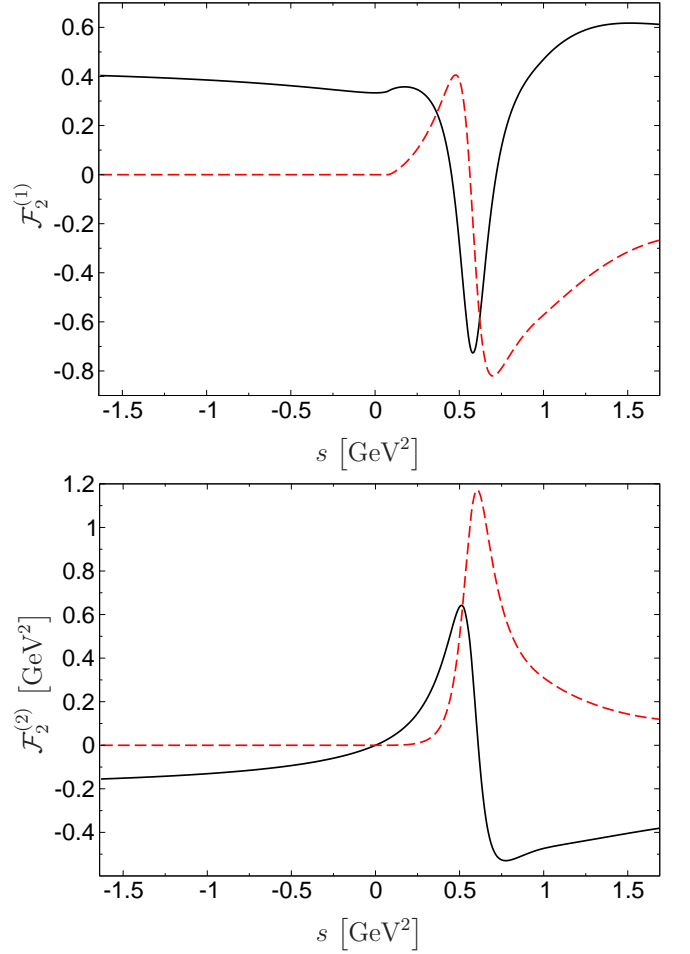


FIG. 2: Basis functions  $\mathcal{F}_2^{(i)}$  for  $\gamma\pi \rightarrow \pi\pi$ . The black solid (red dashed) lines refer to the real (imaginary) parts.

the dispersion relation for  $\mathcal{F}(s)$  can be represented in the form

$$\begin{aligned} \mathcal{F}(s) &= C_2^{(1)}\mathcal{F}_2^{(1)}(s) + C_2^{(2)}\mathcal{F}_2^{(2)}(s) \\ &= \frac{1}{3}(C_2^{(1)} + C_2^{(2)}s) + \frac{1}{\pi} \int_{4M_\pi^2}^{\infty} \frac{ds'}{s'^2} \frac{s^2}{s' - s} \\ &\quad \times (C_2^{(1)}\text{Im}\mathcal{F}_2^{(1)}(s') + C_2^{(2)}\text{Im}\mathcal{F}_2^{(2)}(s')), \end{aligned} \quad (34)$$

where  $C_2^{(i)}$  refer to the subtraction constants in the twice-subtracted dispersion relation. These are the free parameters of the fit. In contrast, the basis functions  $\mathcal{F}_2^{(i)}(s)$  can be calculated once and for all, for a given input of the  $\pi\pi$  phase shift  $\delta_1^1(s)$  (the results for the phase shift from [39] are depicted in Fig. 2). The partial wave  $f_1(s)$  follows from

$$\begin{aligned} f_1(s) &= \frac{3}{4} \int_{-1}^1 dz (1 - z^2) (\mathcal{F}(s) + \mathcal{F}(t) + \mathcal{F}(u)) \\ &= C_2^{(1)} + C_2^{(2)}M_\pi^2 + \frac{1}{\pi} \int_{4M_\pi^2}^{\infty} ds' K(s, s') \\ &\quad \times (C_2^{(1)}\text{Im}\mathcal{F}_2^{(1)}(s') + C_2^{(2)}\text{Im}\mathcal{F}_2^{(2)}(s')), \end{aligned} \quad (35)$$

with integration kernel

$$K(s, s') = \frac{s^2}{s'^2(s' - s)} + \frac{3}{b(s)} \left\{ (1 - x_s^2) Q_0(x_s) + x_s \right\} - \frac{2}{s'} + \frac{s - 3M_\pi^2}{s'^2}, \quad x_s = \frac{s' - a(s)}{b(s)}, \quad (36)$$

and the lowest Legendre function of the second kind

$$Q_0(z) = \frac{1}{2} \int_{-1}^1 \frac{dx}{z - x}, \quad Q_0(z \pm i\epsilon) = \frac{1}{2} \log \left| \frac{1+z}{1-z} \right| \mp i \frac{\pi}{2} \theta(1 - z^2). \quad (37)$$

For the GKPY  $\rho$  parameters from [28] we obtain

$$f_{1,I}(s_\rho) = C_2^{(1)} (0.588(5) + 0.193(7)i) - C_2^{(2)} (0.071(7) + 0.570(5)i) \text{ GeV}^2, \quad (38)$$

where the uncertainties reflect the propagated errors on the pole parameters only (when experiment reaches few-percent accuracy, also the uncertainties in the  $\pi\pi$  phase shift will have to be included). Once the  $C_2^{(i)}$  are fit to cross-section data, this relation determines  $f_{1,I}(s_\rho)$ , and thus, by means of (32), the radiative coupling of the  $\rho(770)$  (including its phase). The current knowledge of these couplings, see (40) below, indicates that, similarly to  $g_{\rho\gamma}$ ,  $g_{\rho\pi\gamma}$  is almost real with the same sign as  $g_{\rho\pi\pi}$ .

#### IV. LINE SHAPE OF $\gamma\pi \rightarrow \pi\pi$

Currently available information on the radiative coupling of the  $\rho(770)$  [6] largely derives from the high-momentum Primakoff experiments [57–59], while no experimental result is available for the  $\rho_3(1690)$  at all. Thanks to its high-statistics data, COMPASS has the unique opportunity to determine these couplings either for the first time or with unprecedented accuracy; compare their results for the radiative widths of the  $a_2(1320)$  and the  $\pi_2(1670)$  as extracted from the similar Primakoff reaction  $\gamma\pi \rightarrow 3\pi$  [60]. For the  $\rho(770)$  such a measurement is intimately related to the determination of the chiral anomaly, and, building upon [19], the previous section establishes the formalism to extract both simultaneously in a consistent, model-independent way.

In this section, we reverse the argument and collect the currently available information to predict the line shape to be expected in the  $\gamma\pi \rightarrow \pi\pi$  cross section. First of all, the combination  $C_2^{(1)} + C_2^{(2)} M_\pi^2$  is related to the chiral anomaly, but only up to an additional quark-mass renormalization

$$C_2^{(1)} + C_2^{(2)} M_\pi^2 = \bar{F}_{3\pi} \equiv F_{3\pi} (1 + 3M_\pi^2 \bar{C}), \quad (39)$$

estimated from resonance saturation to  $3M_\pi^2 \bar{C} = 6.6\%$  [8]. We use the corresponding central value, but,

given that we wish to extract  $\bar{F}_{3\pi}$  from the data, assign a 10% uncertainty,  $\bar{F}_{3\pi} = 10.4(1.0) \text{ GeV}^{-3}$ , to reflect the level of accuracy that previous measurements have established. The second combination of coupling constants corresponds to the radiative coupling of the  $\rho(770)$ , for which we take the  $SU(3)$  VMD result  $|g_{\rho\pi\gamma}| = 0.79(8) \text{ GeV}^{-1}$ , but, in view of the results for the pion form factor in Sect. IIIB, attach a 10% uncertainty as well. These constraints translate into

$$C_2^{(1)} = 9.9(1.0) \text{ GeV}^{-3}, \quad C_2^{(2)} = 24.1(2.5) \text{ GeV}^{-5}, \quad (40)$$

where the uncertainty in  $C_2^{(1)}$  and  $C_2^{(2)}$  is entirely dominated by  $\bar{F}_{3\pi}$  and  $|g_{\rho\pi\gamma}|$ , respectively. For the  $\rho_3(1690)$  we use the parameters as given in Sect. IIB.

The twice-subtracted dispersion relation (34) is perfectly suited to extract the coefficients  $C_2^{(i)}$  from cross-section data up to and including the  $\rho$  resonance, but displays a pathological high-energy behavior. To obtain a description that remains valid in the whole region below 2 GeV, we implement a version of the basis functions  $\mathcal{F}_2^{(i)}$  with a relatively low cut-off parameter  $\Lambda = 1.3 \text{ GeV}$  that leaves the low-energy physics virtually unaffected, but allows us to introduce a high-energy completion of the resulting partial wave  $f_1(s) \sim 1/s$ , in agreement with general arguments based on the Froissart bound [61]. In addition to the  $P$ -wave, the symmetrized version (33) produces non-vanishing contributions to  $f_l(s)$  for all (odd)  $l$  in the partial-wave projection. However, we checked that the corresponding  $F$ - and higher partial waves can be ignored, and similarly effects from excited  $\rho$  states,  $\rho'$  and  $\rho''$ , are likely negligible [32, 62] (assuming that these resonances couple with a comparable relative strength as in the pion form factor [56]). While inelastic corrections included directly in the dispersive description by means of the inelasticity parameter are typically small [33], such excited  $\rho$  states provide an indicator for the size of the dominant inelasticities from  $4\pi$  intermediate states; see also [45].<sup>1</sup> Finally, the narrow-resonance approximation for the  $\rho_3$  is strictly meaningful only at the resonance mass, while the additional momentum dependence in (22) distorts the resonance shape. To obtain a more realistic line shape we follow [63, 64] and introduce centrifugal-barrier factors, which amounts to the replacement

$$f_3^{\text{VMD}}(s) \rightarrow f_3^{\text{VMD}}(s) \frac{B_3(q_f(s)R)B_3(q_i(s)R)}{B_3(q_f(M_{\rho_3}^2)R)B_3(q_i(M_{\rho_3}^2)R)}, \quad (41)$$

with  $B_3(x) = 15/\sqrt{225 + 45x^2 + 6x^4 + x^6}$ , initial- and

<sup>1</sup> We wish to emphasize that our dispersive representation of the  $P$ -wave is very reliable mostly below 1 GeV, and the model for the  $F$ -wave around the  $\rho_3$  resonance. Despite the indications for comparably smaller  $\rho'$ ,  $\rho''$  contributions, we do not claim to make a high-precision prediction of the line shape between 1 and 1.5 GeV.

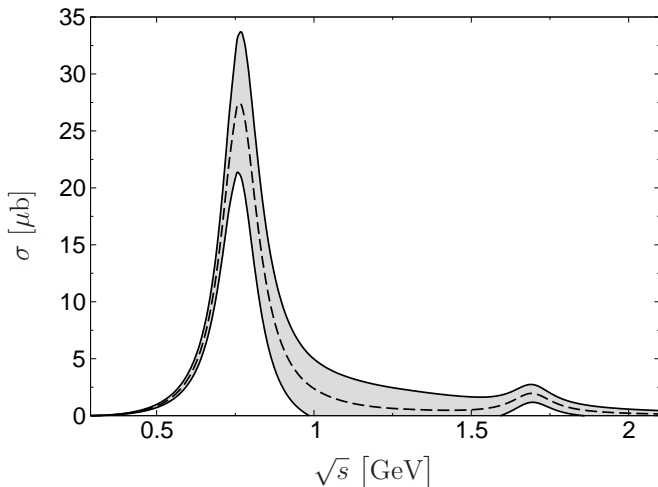


FIG. 3: Total cross section for  $\gamma\pi \rightarrow \pi\pi$ . The dashed line refers to our central solution, using (18) and (40).

final-state momenta

$$q_i(s) = \frac{s - M_\pi^2}{2\sqrt{s}}, \quad q_f(s) = \sqrt{\frac{s}{4} - M_\pi^2}, \quad (42)$$

and a scale  $R \sim 1$  fm. The resulting cross section is shown in Fig. 3. Note in particular that the peak of the  $F$ -wave cross section,

$$\begin{aligned} \sigma_F(M_{\rho_3}^2) &= \frac{3(M_{\rho_3}^2 - 4M_\pi^2)^{3/2}(M_{\rho_3}^2 - M_\pi^2)}{896\pi M_{\rho_3}} |f_3(M_{\rho_3}^2)|^2 \\ &= \frac{56\pi M_{\rho_3}^2}{(M_{\rho_3}^2 - M_\pi^2)^2} \frac{\Gamma_{\rho_3 \rightarrow \pi\pi} \Gamma_{\rho_3 \rightarrow \pi\gamma}}{\Gamma_{\rho_3}^2} \\ &= 1.7(6) \mu\text{b}, \end{aligned} \quad (43)$$

amounts to roughly 6% of the dominant  $\rho(770)$  peak. While currently the uncertainties are large, an improved measurement of the energy dependence would immediately translate to better constraints on the underlying QCD parameters, most notably the chiral anomaly  $F_{3\pi}$ , but also, as we have shown in this paper, the radiative couplings of the  $\rho(770)$  and  $\rho_3(1690)$  resonances.

## V. SUMMARY

Extending the dispersive formalism for  $\gamma\pi \rightarrow \pi\pi$  developed in [19], we have worked out the analytic continuation necessary to extract the radiative coupling of the  $\rho(770)$ , as defined by the residue at its resonance pole. Throughout, we have indicated the correspondence to the parameters that would occur within a narrow-resonance description, and collected the current phenomenological information. Combined with a VMD estimate for the  $\rho_3(1690)$ , we have obtained a prediction for the cross section of  $\gamma\pi \rightarrow \pi\pi$  up to 2 GeV, with uncertainties dominated by the current knowledge of the underlying parameters: the chiral anomaly  $F_{3\pi}$  and the radiative couplings of the  $\rho(770)$  and  $\rho_3(1690)$  resonances.

This prediction can be considered a benchmark for the ongoing Primakoff program at COMPASS. Measuring the cross section with reduced uncertainties compared to Fig. 3 would allow one to test the narrow-width estimate of the  $\rho_3 \rightarrow \pi\gamma$  decay rate,  $\Gamma_{\rho_3 \rightarrow \pi\gamma} = 48(18)$  keV, and to improve the determination of the chiral anomaly and the  $\rho \rightarrow \pi\gamma$  coupling, both without relying on model assumptions while still profiting from the full statistics of the  $\rho$  resonance. Such improved experimental information on  $\gamma\pi \rightarrow \pi\pi$  is particularly timely given its relation to hadronic light-by-light scattering in the anomalous magnetic moment of the muon as well as recent lattice calculations. We look forward to the results of the ongoing analysis of the  $\pi^-\pi^0$  channel at COMPASS that will provide an important step in this direction.

## Acknowledgments

We would like to thank Jan Friedrich, Boris Grube, Misha Mikhasenko, Stephan Paul, Jacobo Ruiz de Elvira, and Julian Seyfried for helpful discussions. Financial support by the DOE (Grant No. DE-FG02-00ER41132) and the DFG (CRC 110 ‘‘Symmetries and the Emergence of Structure in QCD’’) is gratefully acknowledged.

---

[1] J. Wess and B. Zumino, Phys. Lett. **37B**, 95 (1971).  
[2] E. Witten, Nucl. Phys. B **223**, 422 (1983).  
[3] S. L. Adler, B. W. Lee, S. B. Treiman and A. Zee, Phys. Rev. D **4**, 3497 (1971).  
[4] M. V. Terent’ev, Phys. Lett. **38B**, 419 (1972).  
[5] R. Aviv and A. Zee, Phys. Rev. D **5**, 2372 (1972).  
[6] C. Patrignani *et al.* [Particle Data Group], Chin. Phys. C **40**, 100001 (2016).  
[7] Y. M. Antipov *et al.*, Phys. Rev. D **36**, 21 (1987).  
[8] J. Bijnens, A. Bramon and F. Cornet, Phys. Lett. B **237**, 488 (1990).  
[9] B. R. Holstein, Phys. Rev. D **53**, 4099 (1996) [hep-

ph/9512338].  
[10] T. Hannah, Nucl. Phys. B **593**, 577 (2001) [hep-ph/0102213].  
[11] T. N. Truong, Phys. Rev. D **65**, 056004 (2002) [hep-ph/0105123].  
[12] L. Ametller, M. Knecht and P. Talavera, Phys. Rev. D **64**, 094009 (2001) [hep-ph/0107127].  
[13] J. Bijnens, K. Kampf and S. Lanz, Nucl. Phys. B **860**, 245 (2012) [arXiv:1201.2608 [hep-ph]].  
[14] I. Giller, A. Ocherashvili, T. Ebertshauser, M. A. Moinester and S. Scherer, Eur. Phys. J. A **25**, 229 (2005) [hep-ph/0503207].

- [15] I. Larin *et al.* [PrimEx Collaboration], Phys. Rev. Lett. **106** (2011) 162303 [arXiv:1009.1681 [nucl-ex]].
- [16] A. M. Bernstein and B. R. Holstein, Rev. Mod. Phys. **85**, 49 (2013) [arXiv:1112.4809 [hep-ph]].
- [17] R. A. Briceño, J. J. Dudek, R. G. Edwards, C. J. Shultz, C. E. Thomas and D. J. Wilson, Phys. Rev. Lett. **115**, 242001 (2015) [arXiv:1507.06622 [hep-ph]].
- [18] R. A. Briceño, J. J. Dudek, R. G. Edwards, C. J. Shultz, C. E. Thomas and D. J. Wilson, Phys. Rev. D **93**, 114508 (2016) [arXiv:1604.03530 [hep-ph]].
- [19] M. Hoferichter, B. Kubis and D. Sakkas, Phys. Rev. D **86**, 116009 (2012) [arXiv:1210.6793 [hep-ph]].
- [20] M. Hoferichter, B. Kubis, S. Leupold, F. Niecknig and S. P. Schneider, Eur. Phys. J. C **74**, 3180 (2014) [arXiv:1410.4691 [hep-ph]].
- [21] G. Colangelo, M. Hoferichter, M. Procura and P. Stoffer, JHEP **1409**, 091 (2014) [arXiv:1402.7081 [hep-ph]].
- [22] G. Colangelo, M. Hoferichter, B. Kubis, M. Procura and P. Stoffer, Phys. Lett. B **738**, 6 (2014) [arXiv:1408.2517 [hep-ph]].
- [23] G. Colangelo, M. Hoferichter, M. Procura and P. Stoffer, JHEP **1509**, 074 (2015) [arXiv:1506.01386 [hep-ph]].
- [24] G. Colangelo, M. Hoferichter, M. Procura and P. Stoffer, Phys. Rev. Lett. **118**, 232001 (2017) [arXiv:1701.06554 [hep-ph]].
- [25] G. Colangelo, M. Hoferichter, M. Procura and P. Stoffer, JHEP **1704**, 161 (2017) [arXiv:1702.07347 [hep-ph]].
- [26] J. Seyfried, Master's thesis, TU München, 2017.
- [27] G. Colangelo, J. Gasser and H. Leutwyler, Nucl. Phys. B **603**, 125 (2001) [hep-ph/0103088].
- [28] R. García-Martín, R. Kamiński, J. R. Peláez and J. Ruiz de Elvira, Phys. Rev. Lett. **107**, 072001 (2011) [arXiv:1107.1635 [hep-ph]].
- [29] M. Jacob and G. C. Wick, Annals Phys. **7**, 404 (1959) [Annals Phys. **281**, 774 (2000)].
- [30] K. M. Watson, Phys. Rev. **95**, 228 (1954).
- [31] F. Klingl, N. Kaiser and W. Weise, Z. Phys. A **356**, 193 (1996) [hep-ph/9607431].
- [32] M. Zanke, Bachelor's thesis, University of Bonn, 2017.
- [33] F. Niecknig, B. Kubis and S. P. Schneider, Eur. Phys. J. C **72**, 2014 (2012) [arXiv:1203.2501 [hep-ph]].
- [34] T. Maeda, K. Yamada, M. Oda and S. Ishida, Int. J. Mod. Phys. Conf. Ser. **35**, 1460454 (2014) [arXiv:1310.7507 [hep-ph]].
- [35] B. Moussallam, Eur. Phys. J. C **71**, 1814 (2011) [arXiv:1110.6074 [hep-ph]].
- [36] S. M. Roy, Phys. Lett. **36B**, 353 (1971).
- [37] B. Ananthanarayan, G. Colangelo, J. Gasser and H. Leutwyler, Phys. Rept. **353**, 207 (2001) [hep-ph/0005297].
- [38] I. Caprini, G. Colangelo and H. Leutwyler, Eur. Phys. J. C **72**, 1860 (2012) [arXiv:1111.7160 [hep-ph]].
- [39] R. García-Martín, R. Kamiński, J. R. Peláez, J. Ruiz de Elvira and F. J. Ynduráin, Phys. Rev. D **83**, 074004 (2011) [arXiv:1102.2183 [hep-ph]].
- [40] J. Ruiz de Elvira, private communication.
- [41] J. F. de Trocóniz and F. J. Ynduráin, Phys. Rev. D **65**, 093001 (2002) [hep-ph/0106025].
- [42] H. Leutwyler, hep-ph/0212324.
- [43] G. Colangelo, Nucl. Phys. Proc. Suppl. **131**, 185 (2004) [hep-ph/0312017].
- [44] J. F. de Trocóniz and F. J. Ynduráin, Phys. Rev. D **71**, 073008 (2005) [hep-ph/0402285].
- [45] C. Hanhart, Phys. Lett. B **715**, 170 (2012) [arXiv:1203.6839 [hep-ph]].
- [46] B. Ananthanarayan, I. Caprini, D. Das and I. Sentitemsu Imsong, Phys. Rev. D **89**, 036007 (2014) [arXiv:1312.5849 [hep-ph]].
- [47] B. Ananthanarayan, I. Caprini, D. Das and I. Sentitemsu Imsong, Phys. Rev. D **93**, 116007 (2016) [arXiv:1605.00202 [hep-ph]].
- [48] M. Hoferichter, B. Kubis, J. Ruiz de Elvira, H.-W. Hammer and U.-G. Meißner, Eur. Phys. J. A **52**, 331 (2016) [arXiv:1609.06722 [hep-ph]].
- [49] C. Hanhart, S. Holz, B. Kubis, A. Kupść, A. Wirzba and C. W. Xiao, Eur. Phys. J. C **77**, 98 (2017) [arXiv:1611.09359 [hep-ph]].
- [50] M. N. Achasov *et al.*, J. Exp. Theor. Phys. **103**, 380 (2006) [Zh. Eksp. Teor. Fiz. **130**, 437 (2006)] [hep-ex/0605013].
- [51] R. R. Akhmetshin *et al.* [CMD-2 Collaboration], Phys. Lett. B **648**, 28 (2007) [hep-ex/0610021].
- [52] B. Aubert *et al.* [BaBar Collaboration], Phys. Rev. Lett. **103**, 231801 (2009) [arXiv:0908.3589 [hep-ex]].
- [53] F. Ambrosino *et al.* [KLOE Collaboration], Phys. Lett. B **700**, 102 (2011) [arXiv:1006.5313 [hep-ex]].
- [54] D. Babusci *et al.* [KLOE Collaboration], Phys. Lett. B **720**, 336 (2013) [arXiv:1212.4524 [hep-ex]].
- [55] M. Ablikim *et al.* [BESIII Collaboration], Phys. Lett. B **753**, 629 (2016) [arXiv:1507.08188 [hep-ex]].
- [56] M. Fujikawa *et al.* [Belle Collaboration], Phys. Rev. D **78**, 072006 (2008) [arXiv:0805.3773 [hep-ex]].
- [57] T. Jensen *et al.*, Phys. Rev. D **27**, 26 (1983).
- [58] J. Huston *et al.*, Phys. Rev. D **33**, 3199 (1986).
- [59] L. Capraro *et al.*, Nucl. Phys. B **288**, 659 (1987).
- [60] C. Adolph *et al.* [COMPASS Collaboration], Eur. Phys. J. A **50**, 79 (2014) [arXiv:1403.2644 [hep-ex]].
- [61] M. Froissart, Phys. Rev. **123**, 1053 (1961).
- [62] S. P. Schneider, B. Kubis and F. Niecknig, Phys. Rev. D **86**, 054013 (2012) [arXiv:1206.3098 [hep-ph]].
- [63] F. Von Hippel and C. Quigg, Phys. Rev. D **5**, 624 (1972).
- [64] C. Adolph *et al.* [COMPASS Collaboration], Phys. Rev. D **95**, 032004 (2017) [arXiv:1509.00992 [hep-ex]].